Mon. Not. R. Astron. Soc. **000**, 1–11 (2006) Printed 22 May 2008 (MN LaTeX style file v2.2)

arXiv:0708.2702v2 [astro-ph] 22 May 2008

The Mass Assembly of Fossil Groups of Galaxies in the Millennium Simulation

Ali Dariush*[1], Habib G. Khosroshahi[1], Trevor J. Ponman[1], Frazer Pearce[2],
Somak Raychaudhury[1] & Will Hartley[2]
[1]*School of Physics and Astronomy, University of Birmingham, Birmingham B15 2TT, UK*
[2]*School of Physics and Astronomy, University of Nottingham, Nottingham, NG7 2RD, UK*

ABSTRACT

The evolution of present-day fossil galaxy groups is studied in the Millennium Simulation. Using the corresponding Millennium gas simulation and semi-analytic galaxy catalogues, we select fossil groups at redshift zero according to the conventional observational criteria, and trace the haloes corresponding to these groups backwards in time, extracting the associated dark matter, gas and galaxy properties. The space density of the fossils from this study is remarkably close to the observed estimates and various possibilities for the remaining discrepancy are discussed. The fraction of X-ray bright systems which are fossils appears to be in reasonable agreement with observation, and the simulations predict that fossil systems will be found in significant numbers (3-4% of the population) even in quite rich clusters. We find that fossils assemble a higher fraction of their mass at high redshift, compared to non-fossil groups, with the ratio of the currently assembled halo mass to final mass, at any epoch, being about 10 to 20% higher for fossils. This supports the paradigm whereby fossils represent undisturbed, early-forming systems in which large galaxies have merged to form a single dominant elliptical.

Key words: cosmology: theory — galaxies: formation — galaxies: kinematics and dynamics — hydrodynamics — methods: numerical

1 INTRODUCTION

Galaxy groups are believed to play a key role in the formation and evolution of structure in the universe as, within a hierarchical framework, they span the regime between individual galaxies and massive clusters. They are also more varied in their properties than galaxy clusters, as seen when various scaling relations are compared with those of galaxy clusters (Kaiser 1991; Ponman et al. 1996; White et al. 1997; Allen & Fabian 1998; Mulchaey & Zabludoff 1998; Arnaud & Evrard 1999; Xue & Wu 2000; Helsdon & Ponman 2000; Xue et al. 2001; Helsdon & Ponman 2003). For instance, the relation between the luminosity and temperature of the X-ray emitting hot intergalactic medium (the L–T relation) has a larger scatter and a different slope for groups, when compared to similar properties of clusters. Various feedback mechanisms are often invoked to explain these differences. In addition, due to their lower velocity dispersion, groups are rapidly evolving systems, and galaxy mergers within groups can have a more significant effect on these relations than in clusters. In principle, the presence of cool cores and active galactic nuclei (AGN), as well as the star formation history, are all affected by major interactions in the heart of a group or cluster. It would therefore be useful to find a class of groups or clusters with no major mergers in their recent history, to provide a baseline for the evolution of a passive system, with no major disruption.

Fossil groups are good candidates for such a class of objects. They are distinguished by a large gap between the brightest galaxy and the fainter members, with an under-abundance of L_* galaxies. Zabludoff & Mulchaey (1998) suggest that, for an X-ray detected group, the merging timescale for the most luminous group members ($L \approx L_*$) is of order of a few tenths of an Hubble time, in agreement with the numerical simulations. A single giant elliptical galaxy can form as a result of multiple mergers within a few Gyr (Barnes 1989). Thus, it is likely that one can find merged groups in the form of an isolated giant elliptical galaxy with an extended halo of hot gas, since the timescale for gas infall is longer than that on which galaxies merge (Ponman & Bertram 1993). In such systems, the brighter galaxies, which have a relatively shorter merging timescale, are expected to merge earlier leaving the fainter end of the luminosity function intact (Dubinski 1998; Miles et al. 2004).

Following the discovery of a fossil group having the above characteristics from ROSAT observations (Ponman et al. 1994), more fossil systems have been identified (Mulchaey & Zabludoff 1999; Vikhlinin et al. 1999; Jones et al. 2000; Romer 2000;

---

* E-mail: aad@star.sr.bham.ac.uk

Matsushita 2001; Jones et al. 2003). They are generally based on the definition of fossil groups from Jones et al. (2003), i.e. groups with a minimum X-ray luminosity of $L_{\rm X,bol} \approx 0.25 \times 10^{42} h^{-2}$erg s^{-1}, as well as minimum magnitude difference of two between the first and second ranked galaxies, within half the projected radius that encloses an overdensity of 200 times the mean density of the universe (R_{200}). For an NFW profile (Navarro, Frenk & White 1996), this is roughly equivalent to R_{500}, the radius enclosing an overdensity of 500 times the mean (for NFW haloes of the appropriate concentration, $R_{500} \sim 0.59 \times R_{200}$). A few of these fossil groups have been the subject of detailed investigations (Khosroshahi, Jones & Ponman 2004; Yoshioka et al. 2004; Sun et al. 2004; Ulmer et al. 2005; Cypriano, Mendes de Oliveira & Sodré 2006; Mendes de Oliveira, Cypriano & Sodré 2006; Khosroshahi et al. 2006).

While most previous studies have focused on X-ray properties of fossils, there is also emerging evidence that the galaxy properties in fossils are different from those in non-fossils (Khosroshahi, Ponman & Jones 2006). For instance the isophotal shapes of the central fossil galaxies appear to be non-boxy, suggesting that they may have formed in gas rich mergers. Various observational and theoretical studies have suggested a significant fraction of galaxy groups to be fossils (Vikhlinin et al. 1999; Jones et al. 2003; D'Onghia et al. 2005; Milosavljević et al. 2006; Sommer-Larsen 2006), though often the criteria used to define fossils in theoretical work are not easy to relate to observational studies.

Fossils may represent extreme examples of a continuum of group properties – they are consistently found to be outliers in the usual scaling relations involving optical, X-ray and dynamical properties (Khosroshahi, Ponman & Jones 2007). While fossils fall on the L-T relation of non-fossil groups and clusters, they appear to be both hotter and more X-ray luminous than non-fossils of the same mass. Cooler fossil groups also show lower entropy than their non-fossil counterparts. According to Khosroshahi, Ponman & Jones (2007), the haloes of fossil groups appear to be more concentrated than those of non-fossil systems, for a given mass, which suggests that fossils have an early formation epoch. As such, we have much to learn from them, and the investigation of objects with similar properties in cosmological simulations can provide important insights into the physical processes that underly the scaling relations. It can also reveal limitations in the numerical simulations, related to the treatment of physical effects like pre-heating, feedback and merging, which are difficult to model. It is thus important to study the formation and evolution of these systems in the cosmological N-Body simulations which have become essential tools for studying formation of large scale structure in the Universe.

In this paper we use the Millennium simulation (Springel et al. 2005) together with the semi-analytic models (Croton et al. 2006) of galaxy formation within dark matter haloes and the Millennium gas simulation (Pearce et al. 2007), to identify fossil groups, study their properties in the simulations and make a comparison to the observations. We begin with a brief discussion in §2 of the Millennium Simulation, and the implemented semi-analytic galaxy catalogues and gas simulations. In §3 we discuss our method of identifying *optical* and *X-ray* fossil groups from these catalogues. In §4, we discuss the various properties of these fossil groups, their abundance in the local Universe and the evolution of simulated X-ray fossils with time. Finally, in §5, we summarize the implications of our results in terms of the evolution of fossil groups in the context of multiwavelength observations. Throughout the paper we adopt $H_0 = 100\, h$ km s^{-1} Mpc^{-1} for the Hubble constant.

2 DESCRIPTION OF THE SIMULATIONS

In order to extract fossil groups in the Millennium simulation, using observational selection criteria, we require a simulation suite that includes the baryonic physics of hot gas and galaxies, as well as a high resolution dark matter framework and a sufficient spatial volume to limit the effects of cosmic variance. For this study we use the dark matter Millennium Simulation (Springel et al. 2005), a 10-billion particle model of a comoving volume of side $500h^{-1}$ Mpc, on top of which a publicly available semi-analytic galaxy model (Croton et al. 2006) has been constructed. For the hot gas we have repeated the Millennium simulation with a lower resolution simulation including gas physics utilising the same volume, phases and amplitudes as the original dark-matter-only model. This run accurately reproduces the structural framework of the Millennium Simulation (Pearce et al. 2007). Below we summarize the main characteristics of the above simulations.

2.1 The Millennium Simulation

The Millennium Simulation is based on a Cold Dark Matter cosmological model of structure formation, with a Dark Energy field Λ. The basic assumptions are those of an inflationary universe, dominated by dark matter particles, leading to a bottom-up hierarchy of structure formation, via collapsing and merging of small dense haloes at high redshifts, into the large virialised systems such as groups and clusters that contain the galaxies that we observe today. The simulation was performed using the publicly available parallel TreePM code Gadget2 (Springel et al. 2001), achieving a 3D dynamic range of 10^5 by evolving 2160^3 particles of individual mass $8.6 \times 10^8 h^{-1}$ M$_\odot$, within a co-moving periodic box of side $500h^{-1}$ Mpc, and employing a gravitational softening of $5h^{-1}$ kpc, from redshift $z = 127$ to the present day. The cosmological parameters for the Millennium Simulation were: $\Omega_\Lambda = 0.75, \Omega_M = 0.25, \Omega_b = 0.045, h = 0.73, n = 1$, and $\sigma_8 = 0.9$, where the Hubble constant is characterised as $100\, h\, {\rm km s^{-1} Mpc^{-1}}$. These cosmological parameters are consistent with recent combined analysis from *WMAP* data (Spergel et al. 2003) and the 2dF galaxy redshift survey (Colless et al. 2001), although the value for σ_8 is a little higher than would perhaps have been desirable in retrospect.

The derived dark matter halo catalogues include haloes down to a resolution limit of 20 particles, which yields a minimum halo mass of $1.72 \times 10^{10} h^{-1}$ M$_\odot$. Haloes in the simulation are found using a friends-of-friends (FOF) group finder, tuned to extract haloes with overdensities of at least 200 relative to the critical density. Within a FOF halo, substructures or subhaloes are identified using the SUBFIND algorithm developed by Springel et al. (2001), and the treatment of the orbital decay of satellites is described in the next section.

During the Millennium Simulation, 64 time-slices of the locations and velocities of all the particles were stored, spread approximately logarithmically in time between $z = 127$ and $z = 0$. From these time-slices, merger trees are built by combining the tables of all haloes found at any given output time, a process which enables us to trace the growth of haloes and their subhaloes through time within the simulation.

2.2 The Semi Analytic model

Using the dark matter haloes of the Springel et al. (2005) simulation, Croton et al. (2006) have simulated the growth of galaxies, and their central supermassive black holes, by self-consistently implementing semi-analytic models of galaxies on the outputs of the Millennium Simulation. The semi-analytic catalogue contains 9 million galaxies at $z = 0$ down to a limiting absolute magnitude of $M_R - 5\log\, h = -16.6$, observed in B, V, R, I and K filters. The models focus on the growth of black holes and AGNs as feedback sources. The inclusion of AGN feedback in the semi-analytic model (which allows the cooling flow to be suppressed in massive haloes that undergo quasi-static cooling) and its good agreement with the observed galaxy luminosity function, colour distribution and the clustering properties of galaxies, make this catalogue well-matched and suitable for our study of fossil systems.

In the semi-analytic formulation, galaxies initially form within small dark matter haloes. As the simulation evolves, such a halo may fall into a larger halo. The semi-analytic galaxy within this halo then becomes a satellite galaxy within the main halo and follows the track of its original dark matter halo (now a subhalo) until the mass of the subhalo drops below $1.72{\times}10^{10}h^{-1}$ $\mathrm{M}_{\odot}$, which corresponds to a 20-particle limit in the Millennium Simulation. At this point the galaxy is assumed to spiral into the centre, on some fraction of the dynamical friction timescale, where it merges with the central galaxy of the larger halo (Croton et al. 2006).

2.3 The Millennium Gas Simulation

The Millennium Gas Simulations are a suite of hydrodynamical models, utilising the same volume, and values of initial perturbation amplitudes and phases as the parent dark-matter-only Millennium Simulation. Each of the three models completed to date contains additional baryonic physics: The first does not follow the effects of radiative cooling and so overpredicts the luminosities of group-scale objects significantly. The second includes a simple preheating scheme that is tuned to match the observed X-ray properties of clusters at the present day and the third includes a simple feedback model that matches the observed properties of clusters today, as well as having some chance of following the time evolution. We have used the second of these models in this work, as we only utilise the hydrodynamical properties of the groups at $z = 0$, where the observational and simulation results are well matched.

Each of the Millennium Gas Simulations consists of 5×10^8 particles of each species, resulting in a dark matter mass of $1.422 \times 10^{10}h^{-1}$ $\mathrm{M}_{\odot}$ per particle and a gas mass of $3.12 \times 10^9 h^{-1}$ $\mathrm{M}_{\odot}$ per particle. The Millennium Simulation has roughly 20 times better mass resolution than this and so some perturbation of the dark matter halo locations is to be expected. In practice the position and mass of dark matter haloes above $10^{13}h^{-1}$ $\mathrm{M}_{\odot}$ are recovered to within $50\,h^{-1}$kpc between the two volumes, allowing straightforward halo-halo matching in the large majority of cases.

The Millennium gas simulations used exactly the same cosmological parameters as those stated above. With the inclusion of a gaseous component, additional care needs to be taken in choosing the gravitational softening length in order to avoid spurious heating (Steinmetz & White 1997). We use a comoving value of $25(1 + z)h^{-1}$ kpc, roughly 4% of the mean interparticle separation (Borgani et al. 2006) until $z = 3$, above which a maximum comoving value of $100h^{-1}$ kpc pertains. We have adopted a different output strategy for the Millennium Gas Simulations, preferring to output uniformly in time with an interval roughly corresponding to the dynamical time of objects of interest. This strategy results in 160 rather than 64 outputs and places particular emphasis on the late stages of the simulation.

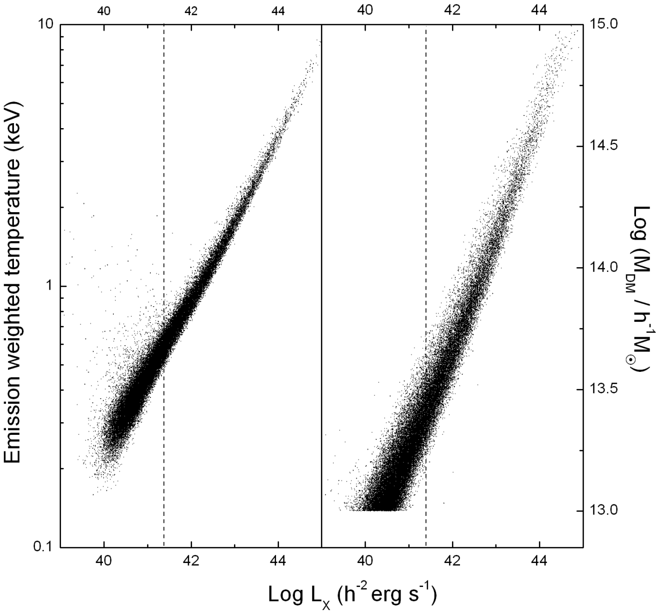

Figure 1. The bolometric X-ray luminosity versus dark matter halo temperature (*left panel*) and mass within R_{200} (*right panel*) for all haloes in the Millennium gas simulation. The vertical dashed lines correspond to the X-ray luminosity threshold $L_{\mathrm{X,bol}} = 0.25 \times 10^{42}\,h^{-2}$erg s^{-1} adopted in this paper for defining fossil groups. The cutoff $M(R_{200}) \geqslant 10^{13}\,h^{-1}$ $\mathrm{M}_{\odot}$ is adopted in § 3.2.

3 SAMPLE SELECTION

3.1 Definition of fossils

Fossil groups are selected according to a combination of X-ray and optical criteria, based on the observational definition given by Jones et al. (2003), which is widely followed in the literature. Their X-ray luminosity must satisfy $L_{\mathrm{X,bol}} \geqslant 0.25 \times 10^{42}h^{-2}$erg s^{-1}, and the difference between the R-band magnitudes of the first and second ranked galaxies, within half the projected radius enclosing 200 times the mean density (R_{200}), must be $\Delta m_{12} \geqslant 2$ magnitudes. A limit of 0.5R_{200} is used because L_* galaxies within this radius should spiral into the centre of the group due to orbital decay by dynamical friction within a Hubble time (Jones et al. 2003). The limit on the bolometric X-ray luminosity $L_{\mathrm{X,bol}}$ helps to exclude poor groups and individual galaxies with a few small satellites. Such groups are often not in dynamical equilibrium, and in addition there might be a gap in their galaxy luminosity function simply as a result of the small numbers of galaxies involved. We address this issue in § 3.3.

3.2 Selection of Fossil galaxies

For this investigation, we first selected dark matter haloes from the Millennium Gas Simulation with masses $M(R_{200}) \geqslant 10^{13}\,h^{-1}\,\mathrm{M}_{\odot}$. As Fig. 1 demonstrates, all haloes for which $L_{X,bol} \geqslant 0.25 \times 10^{42}\,h^{-2}$erg s^{-1} are expected to be included in this sample and thus our fossil sample will be complete. A bolometric

X-ray luminosity of $0.25 \times 10^{42}\ h^{-2}$ erg s^{-1} corresponds to a temperature of $T \approx 0.5$ keV. This constraint on the halo masses results in an initial sample of 51538 dark matter haloes, within which we search for fossil groups.

In order to extract information about dark matter and galaxy properties, for each of these 51538 haloes found in the Millennium Gas Simulation, the counterpart in the Millennium Simulation needs to be found. This is a straightforward procedure because the simulated volume and the amplitudes and phases of the initial power spectrum were matched. However, the dark-matter-only Millennium Simulation has 20 times the mass resolution of the corresponding Millennium Gas Simulation and so contains some additional small scale power. This leads to small offsets (typically around twice the gravitational softening length) in the final coordinates of equivalent haloes, and even smaller mass differences (typically less than 5%). Of the 51538 haloes, 48774 ($\sim$95%) have corresponding haloes identified in the Millennium Simulation. For each of these matched haloes we extracted the coordinates and $BVRIK$ magnitudes for each galaxy contained within R_{200}, from the publically available catalogue of Croton et al. (2006).

The simulated properties of the galaxies occupying each dark matter halo were then used to calculate Δm_{12}, i.e. the difference in R-band magnitude of the first and second ranked galaxies within $0.5R_{200}$ of the centre of the halo. Out of the 48774 matched haloes, 6502 are found to be *optical fossil groups*, i.e. haloes with $\Delta m_{12} \geqslant 2$ mag, among which 1300 are *X-ray fossil groups*, i.e. optical fossil groups with $L_{X,bol} \geqslant 0.25 \times 10^{42}\ h^{-2}$ erg s^{-1}. As can be seen from Fig. 2, X-ray fossil groups do not form a separate population but are rather extreme examples of a smooth distribution. It is also clear that the spread in Δm_{12} increases dramatically with decreasing in the X-ray luminosity and hence the enclosed mass, in agreement with the conditional luminosity function (CLF) formalism of van den Bosch et al. (2007).

Control groups are necessary for our study in order to allow us to compare the properties of X-ray fossil and non-fossil groups. We define two control group samples, based on the magnitude difference of the two brightest members of the group (within $0.5R_{200}$ of the centre of the dark matter halo): (i) $0.8 \leqslant \Delta m_{12} \leqslant 1.0$, and (ii) $0.1 \leqslant \Delta m_{12} \leqslant 0.3$. While members of the former are examples of intermediate groups, the latter could be regarded as a class of extreme non-fossil groups in that they contain at least two galaxies of very similar magnitude. The bolometric X-ray luminosity limit for each of the control samples is the same as that of the X-ray fossil group sample (see Fig. 2).

3.3 The likelihood of finding groups with $\Delta m_{12} \geqslant 2$ at random

One of the central criteria used to define fossils is the absence of galaxies within a range of two magnitudes of the brightest galaxy ($\Delta m_{12} \geqslant 2$). However, for groups with only a small number of members, there is a significant probability of obtaining such a luminosity gap as a natural consequence of the high-end tail of the galaxy luminosity distribution. To quantify the likelihood of obtaining a value of $\Delta m_{12} \geqslant 2$ by chance, Jones et al. (2003) performed 10^4 Monte Carlo simulations for groups and clusters with absolute magnitudes selected at random from a Schechter function (Schechter 1976). Using the parameters of the composite luminosity function of MKW/AWM clusters (Yamagata & Maehara 1986), they found that for the systems of $\sim$40 galaxies, 0.4$\pm$0.06% of the generated luminosity functions had $\Delta m_{12} \geqslant 2$.

We performed a similar analysis for groups spanning a range in richness, and using parameters appropriate to our data from the Millennium simulation. For twenty classes of groups, containing 10, 15, 20, 25,... galaxies respectively, we randomly generated galaxies according to a Schechter luminosity function. (None of our X-ray fossil groups from the Millennium simulation contain fewer than 10 galaxies.) The characteristic magnitude M$_*$ ~ -22.1 and faint-end exponent $\alpha \sim -1.19$, were adopted from a fit of the Schechter function to the R-band luminosity function of the semi-analytic catalogue. A magnitude cut off of -17.4 was then applied to the magnitude of generated galaxies as this is the R-band magnitude completeness limit of the semi-analytic catalogue. 10^6 simulations were carried out for each richness class of group.

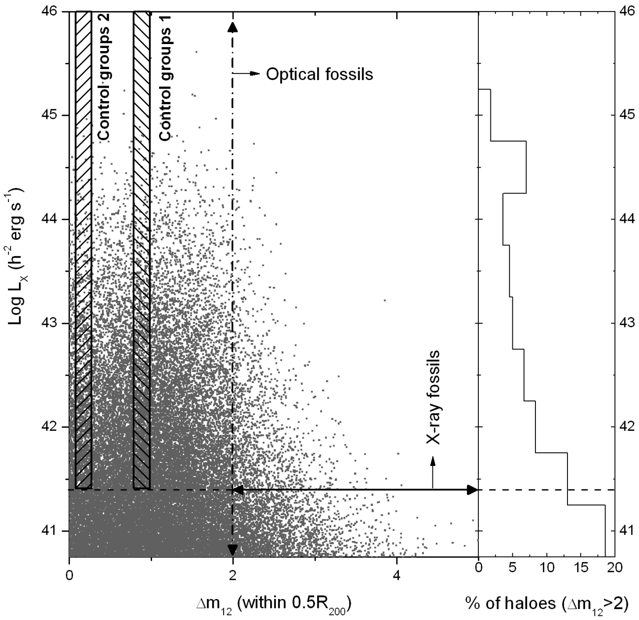

Figure 2. X-ray luminosity versus the R-band luminosity gap Δm_{12} within $0.5R_{200}$ for each of the dark matter haloes with gas properties. The horizontal dashed-line intersects the vertical axis at $L_{X,bol} = 0.25 \times 10^{42} h^{-2}$erg s^{-1}. The top-right part of the graph shows the region for which $\Delta m_{12} \geqslant 2$ mag and $L_{X,bol} \geqslant 0.25 \times 10^{42} h^{-2}$erg s^{-1}, the optical and X-ray criteria that jointly define fossil groups. The two shaded regions show the location of our control samples (see § 3.2 for details). The histogram shows the fraction of optical fossils in each bin of $L_{X,bol}$.

Fig. 3 compares the percentage of optical and X-ray fossil groups from the Millennium simulation as a function of number of galaxies within $0.5R_{200}$ for each dark matter halo, with those populated using a Schechter luminosity function as detailed above. The lower panel shows the result when the expected number of randomly generated groups with $\Delta m_{12} \geqslant 2$, is subtracted from the optical fossils. For poor systems, the incidence of ‘statistical fossils’ is significant. It can be seen that approximately one third of the fossil systems with fewer than 25 galaxies seen in the Millennium data can be attributed to statistical chance (as opposed to the result of physical processes generating a non-statistical luminosity gap). However, even after these random fossils are removed, the fraction of optical fossils increases as the number of galaxies within dark matter haloes decreases. In contrast, for X-ray fossils, many of the poor haloes which qualify as ’statistical fossils’ fail to pass the X-ray luminosity threshold criterion, so the chance fraction is never much larger than 20%. We return to this issue in Sec. 4.1.2. For groups with more than 30 galaxies, the fraction of fossils meeting

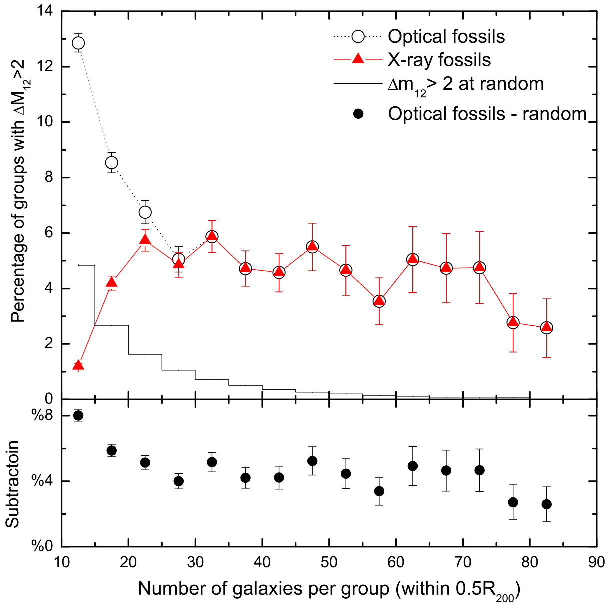

Figure 3. The histogram shows the incidence rate of $\Delta m_{12} \geqslant 2$ occurring by chance from a random population of galaxies selected from a Schechter luminosity function in comparison to fraction of optical fossils (*open circles*) and X-ray fossils (*solid triangles*) in the Millennium simulation, as a function of number of galaxies per halo within $0.5R_{200}$. The lower panel plot (*filled circles*) shows the result of subtracting random groups from the optical fossil groups.

the $\Delta m_{12} \geqslant 2$ criterion by chance drops below 1.0%, and soon becomes negligible.

4 RESULTS

4.1 The Luminosity Gap Statistic

If galaxies in groups and clusters merge with the central galaxy over a finite time to produce a progressively greater massive central galaxy, then one way to quantify the dynamical age of a galaxy system is to measure the luminosity gap between the two most luminous galaxies remaining in the group, provided that there is no infall of bright galaxies from other nearby systems. A relaxed X-ray morphology in observed fossils is an indication of the absence of such a process. Within such a merging scenario for the formation of the brightest group galaxy, the luminosity gap distribution depends on the halo merger rates. This has previously only been examined in analytical studies (Bond et al. 1991), or in large-scale cosmological simulations without a hot baryonic component. Thus, while an important observational criterion for defining fossils relies on the X-ray properties of the group, this has not previously been implemented within the models.

4.1.1 The R-band magnitude gap distribution

Here we compare the luminosity gap distribution between the luminous galaxies found at the centre of dark matter haloes extracted from the Millennium simulation with expectations from the analytical model of Milosavljević et al. (2006), and with observational properties from SDSS clusters.

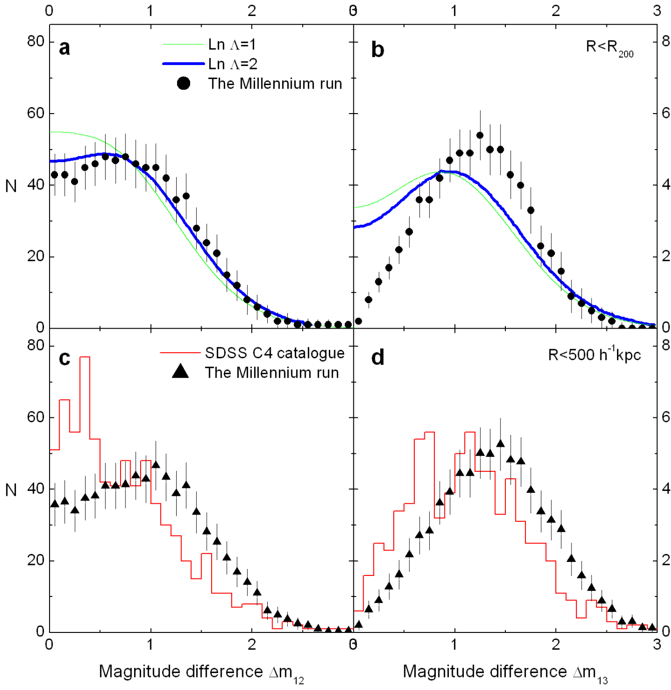

Figure 4. The R-band luminosity gap distribution for haloes from the Millennium semi-analytic model within the mass range $M = 0.5 - 10 \times 10^{14}\, h^{-1}\, \mathrm{M}_{\odot}$, evaluated relative to the first and second most luminous galaxies and the first and the third most luminous galaxies, superposed on the theoretical model of Milosavljević et al. (2006) and the SDSS data for the same mass range but different searching radius (R_{200} for the model and projected radius of $500h^{-1}$kpc for the SDSS data). The Millennium data are plotted within R_{200} (*closed circles*) as well as the projected radius of $500h^{-1}$kpc (*triangles*). (a), (b): The luminosity gap statistic predictions of the theoretical model of Milosavljević et al. (2006) with $\ln \Lambda = 1$ (*thin green line*) and $\ln \Lambda = 2$ (*thick blue line*). (c), (d): The r-band luminosity gap distribution from 730 clusters (*red histogram*) in the SDSS C4 Catalogue of Miller et al. (2005).

Milosavljević et al. (2006) compared the distribution of the predicted luminosity gaps from their analytical model within R_{200}, as a function of halo mass, with the observed luminosity gaps in the SDSS (DR4) clusters (Miller et al. 2005), ranging in mass and redshift from $M = 0.5\text{–}10 \times 10^{14}\, h^{-1}\, \mathrm{M}_{\odot}$ and z=0.02 to 0.17, respectively, within a projected physical radius of 500 h^{-1}kpc. Halo merger rates in their model have been analytically estimated according to the excursion-set theory of Bond et al. (1991), which is also known as the extended Press-Schechter formalism. Assuming a halo density profile of the form of Navarro, Frenk & White (1996), a subhalo of mass m merges into a primary halo of mass M ($m \geqslant \frac{1}{2}M$) and makes a composite halo. As the centre of the subhalo crosses the virial radius of the new composite halo, a merger happens. Then the subhalo spirals toward the centre of the composite halo in a near circular orbit, experiencing dynamical friction.

For comparison with the above study, we evaluate the R-band luminosity difference between the first and second most luminous (Δm_{12}) and the first and the third most luminous (Δm_{13}) galaxies in our Millennium data within R_{200} and within 500 h^{-1}kpc. In Fig. 4, we plot the R-band luminosity gap distribution of the Millennium simulation for the same mass range as the models, together with the luminosity gap distribution of 730 SDSS C4 clusters (Miller et al. 2005). Figs. 4a and 4b compare the predicted gap statistics from Milosavljević et al. (2006) for two values of the Coulomb logarithm, $\ln\Lambda = 1$ and $\ln\Lambda = 2$, within R_{200}. Since the parameter $\ln\Lambda$ is proportional to the force of dynamical friction between the centres of subhalo and primary halo during the process of merging, a higher value of $\ln\Lambda$ corresponds to a faster effective halo merger rate. In numerical simulations, $\ln\Lambda$ is approximated by b_{max}/b_{min}, where b_{max} and b_{min} are the maximum and minimum impact parameters respectively, and $\ln\Lambda$ is expected to be $\sim 1-4$ (Velázquez & White 1999; Fellhauer et al. 2000; D'Onghia et al. 2005). However, in the semi-analytic galaxy catalogues (Croton et al. 2006), based on the Millennium simulation, used in this work, the above relation is approximated by $\ln\Lambda = \ln(1 + M_{200}/m_{\rm sat})$, where m_{sat} is the halo mass of the satellite galaxy.

Within the mass range of the SDSS data there are 8842 haloes in the Millennium simulation catalogue. Accordingly, in Fig. 4, our data have been normalised to be comparable with the SDSS data and the theoretical model of Milosavljević et al. (2006). However, the simulation data is, unlike the observations, complete and uncontaminated by spurious groups or foreground and background galaxies. All these effects are likely to be heavily dependent on the number of galaxies residing in the halo. As such, the comparison with the SDSS data shown in Fig. 4 should be treated with caution.

Given this caveat, our analysis based on the Millennium simulation catalogues agrees remarkably well with the models of Milosavljević et al. (2006) based on the SDSS survey for the luminosity gap distribution of the two brightest galaxies in each of the dark matter haloes, particularly for $\ln\Lambda = 2$ (Fig. 4a). However, for the R-band luminosity gap between the brightest and third brightest galaxies in each system (Fig. 4b), the simulations significantly depart from the model. When comparing with the SDSS data (Figs. 4c and 4d), the simulations overpredict the frequency of groups. The simulations and the SDSS data have similar shaped distributions for the luminosity gap Δm_{13}, but with a shift of ~0.5 mag toward higher Δm_{13} in the simulated haloes.

We emphasize that the Millennium predictions for the luminosity gap statistic are sensitive to the assumed mass range and search radius of dark matter haloes within which brightest halo members are identified. SDSS cluster masses have been estimated from total r-band luminosities, so any inaccuracies in this procedure would affect the comparison with the Millennium data.

Observationally there is an excess population of groups with a small luminosity gap between the first and second ranked galaxies, above what is predicted by the theoretical models or the simulations. This excess population is likely to result from contamination of observed group samples by local structure alignments, and renormalising to a sample without these groups scales down the "Millennium" distribution in Fig. 4c, bringing the simulation results and the observational measurements into better agreement. Results are similar in the K-band.

4.1.2 *The abundance of fossil groups*

The probability of finding fossil systems is expected to increase with decreasing halo mass, as shown in previous studies based on theoretical models or hydrodynamical simulations (D'Onghia et al. 2005; Milosavljević et al. 2006; Sommer-Larsen 2006; van den Bosch et al. 2007). Unfortunately, it is difficult to compare the results from different studies (both theoretical and observational), since they have used a range of search radii (from R_{180} to R_{337} – see Table. 1) within which the $\Delta m_{12} \geqslant 2\,$mag criterion is imposed. Clearly, the larger the search radius, the more demanding is the requirement on the galaxy contents of the system, and the smaller the fraction of groups which will qualify as fossils.

In Fig. 5, the rates of incidence, $P_f(M)$, of optical fossils and X-ray fossils (using our preferred search radius of $0.5R_{200}$, following Jones et al. (2003)) are plotted, as a function of the mass M of the halo, together with the predicted values from the models of Milosavljević et al. (2006) for two values of Λ. The shape of our curve for optical fossils is quite similar to the theoretical models (which included no X-ray luminosity criterion), but the latter actually employed a search radius of R_{200}. To see the effect of this, we also show our Millennium results for this larger search radius. The fraction of fossil systems falls by approximately a factor of 2, when this more demanding requirement is imposed, and so lies significantly below that predicted by Milosavljević et al. (2006).

On scales of $M \sim 10^{13} - 10^{14}h^{-1}{\rm M}_{\odot}$, ~5%–18% of groups are optical fossils. This probability falls to ~3%–5% for more massive ($M \geqslant 10^{14}h^{-1}{\rm M}_{\odot}$) fossil systems. For halo masses $> 5 \times 10^{13}h^{-1}{\rm M}_{\odot}$ all optical fossils in the simulation are also X-ray fossils. However, at the lowest halo masses the fraction of X-ray fossils drops steeply, since many low mass haloes do not satisfy the L_X threshold criterion.

In Table. 1, we summarize the incidence rates of fossil systems from present study as well as those found in the literature. Comparison between these different estimates is difficult, since both the search radius and the halo mass range varies considerably from study to study. However, a direct comparison with the only *observational* estimate (from Jones et al. (2003)) is possible, since we have used the same definitions of fossil groups as these authors. Based on a comparison with the integrated local X-ray luminosity function of Ebeling et al. (2001), Jones et al. (2003) estimated that X-ray fossil systems constitute 8-20% of all systems of the same X-ray luminosity ($L_{X,bol} \geqslant 0.25 \times 10^{42}h^{-2}$erg s^{-1}). The right panel histogram of Fig. 2 represents the fraction of optical fossil systems in each bin of $L_{X,bol}$. Integrating this over all X-ray luminosities above the threshold value for fossils, we find that $\sim 7.2 \pm 0.2\%$ of haloes with $L_{X,bol} \geqslant 0.25 \times 10^{42}h^{-2}$erg s^{-1} are X-ray fossils, which is reasonably consistent with the lower limit of $\sim 8\%$, derived by Jones et al. (2003).

In comparison, detailed hydrodynamical simulations by D'Onghia et al. (2005) and Sommer-Larsen (2006) of 12 galaxy groups, predict a larger fraction of 33%±16% for fossil systems of mass $10^{14}h^{-1}{\rm M}_{\odot}$ or larger. This may be because it is easy to overestimate the local viscosity in hydrodynamic simulations (Tittley et al. 2001), a process that would lead to central overmerging in the models.

4.2 The Space Density of X-ray Fossil Groups

So far, the integrated space density of X-ray fossil groups has been studied for small samples, each of three to five X-ray fossil systems, at different limiting luminosities (Vikhlinin et al. 1999; Romer 2000; Jones et al. 2003). Here, we estimate the space density by systematically counting the fossil groups in the whole 500 h^{-1} Mpc survey volume of the Millennium Simulation at $z = 0$. For comparison with previous studies, we select and count X-ray fossil groups for three limiting X-ray luminosities ranging from 0.25–5$\times10^{42}$ h^{-2}erg s^{-1}. The space densities calculated at different limiting luminosities as well as those from previous studies are given in Table 2. The value from Romer et al is a very rough esti-

Table 1. The incidence rates of fossil systems.

Mass range (h^{-1}M$_\odot$)	L_X ($10^{42}h^{-2}$ erg s^{-1})	Fossil type [a]	Search radius	Fossil fraction (%)	Reference[b]
$\sim 10^{13} - 10^{14}$	-	O	R_{200}	$\sim 5 - 40$	M06
$\sim 10^{13} - 10^{14}$	-	O	R_{180}	$\sim 3.6 \pm 0.1$	vdB07[c]
$\geqslant 10^{14}$	-	O	R_{200}	$\sim 1 - 3$	M06
$\sim 10^{14} - 10^{15}$	-	O	R_{180}	$\sim 6.5 \pm 0.1$	vdB07
$\sim 10^{14}$	-	O	R_{337}	$\sim 33 \pm 16$	SL06, DO05[d]
$\sim 10^{13} - 10^{15}$	-	O	1 h^{-1}Mpc	$\sim 8 - 10$	S07[e]
-	$\geqslant 0.25$	X	$0.5R_{200}$	$\sim 8 - 20$	J03
-	$\geqslant 0.25$	X	$0.5R_{200}$	$\sim 7.2 \pm 0.2$	Present study[f]
$\sim 10^{13} - 10^{15}$	-	O	$0.5R_{200}$	$\sim 13.3 \pm 0.2$	Present study

[a] O: Optical fossils , X: X-ray fossils.

[b] S07: Sales et al. (2007); M06: Milosavljević et al. (2006); vdB07: van den Bosch et al. (2007); SL06: Sommer-Larsen (2006); DO05: D'Onghia et al. (2005); J03: Jones et al. (2003).

[c] Based on the conditional luminosity function (CLF) formalism of van den Bosch et al. (2007).

[d] From hydrodynamical simulations of 12 galaxy groups.

[e] Based on the Millennium simulation. The first brightest galaxies of fossils in their sample are always brighter than $M_R = -20.5$.

[f] Histogram on the right panel of Fig. 2, gives the fraction of X-ray and optical fossils in each bin of L_X.

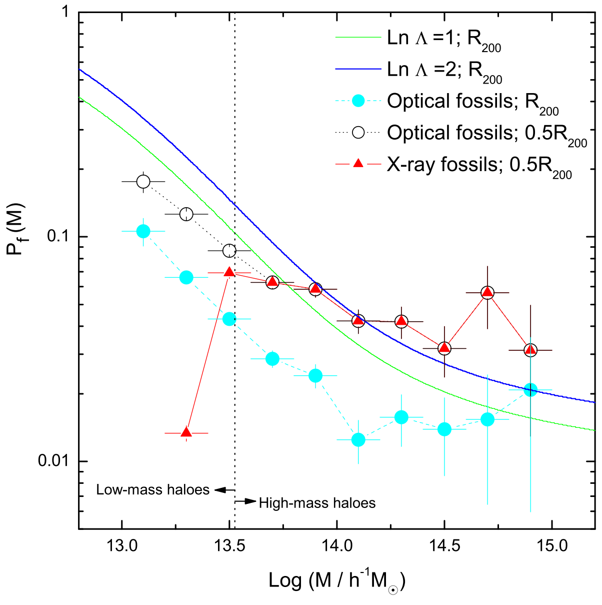

Figure 5. The probability, $P_f(M)$, that a dark matter halo of mass M contains an X-ray fossil group (*closed triangles*), optical fossil group within $0.5R_{200}$ (*open circles*), or optical fossil group within R_{200} (*closed circles*) from the Millennium simulation. The fossil incidence rate from the analytical study of Milosavljević et al. (2006) for two values of $\mathrm{Ln}\Lambda = 1$ (*green line*) and $\mathrm{Ln}\Lambda = 2$ (*blue line*) is also plotted. The vertical dotted-line corresponds to halo mass $\sim 3.34 \times 10^{13}$ h^{-1} M$_\odot$ (see Sec. 4.3).

Table 2. Space densities of fossil galaxy groups.

L_X[a]	N_f[b]	Density[c]	Reference[d]	Present study[c]
> 0.25	5	320^{+216}_{-144}	J03	104 ± 3
> 2.5	3	$16^{+15.2}_{-8.8}$	J03	22.4 ± 1.3
> 2.5	4	$36.8^{+47.2}_{-18.4}$	V99	22.4 ± 1.3
> 2.5	3	~ 160	R00	22.4 ± 1.3
> 5.0	4	$19.2^{+24.8}_{-9.6}$	V99	12.8 ± 1.0

[a] In units of $10^{42}h^{-2}$ erg s^{-1}

[b] Number of fossils

[c] In units of $10^{-7}h^3$ Mpc^{-3}

[d] V99:Vikhlinin et al. (1999), R00:Romer (2000), J03:Jones et al. (2003)

mate, since no redshifts for galaxies surrounding the central object were available in this study.

Our values show that for X-ray luminosities exceeding 2.5-5$\times 10^{42}$ h^{-2}erg s^{-1}, the space density of fossils in the Millennium simulation agrees within the errors with those estimated by Vikhlinin et al. (1999) and Jones et al. (2003). At the lowest X-ray luminosities, the density from the Millennium simulations appear to be lower than observed, though the observational values given in Table 2 have large uncertainties due to the small number of X-ray fossil groups and the effects of cosmic variance. Recent studies of Khosroshahi, Ponman & Jones (2007) and Jeltema et al. (2006) show that one of the fossils in the sample of Jones et al. (2003) does not satisfy the fossil criterion of $\Delta m_{12} \geqslant 2$, which reduces the observational space density. Certainly the number of X-ray fossils found is heavily dependent on the X-ray luminosity threshold chosen and may be influenced by the scatter in X-ray group properties near this lower limit.

4.3 Evolution of Fossil Groups

Strong interactions and mergers between galaxies occur more efficiently in the low velocity dispersion environment of galaxy groups (Miles et al. 2004). Therefore in old, relatively isolated groups, most massive galaxies have sufficient time to merge via dynamical friction. If X-ray fossil groups are indeed systems that formed at an earlier epoch, we should be able to verify this from the merger histories of present-day fossils in the Millennium simulation: an

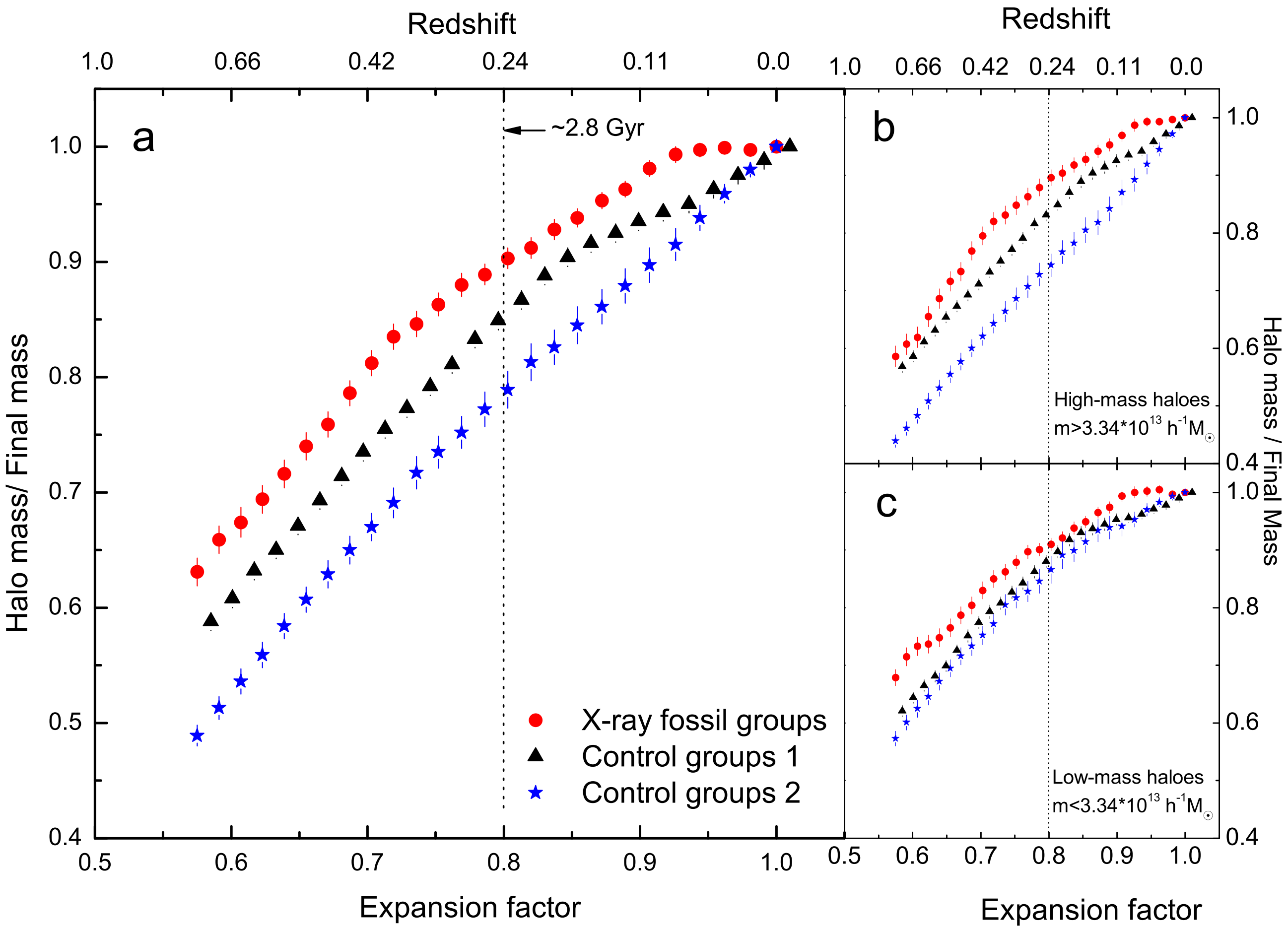

Figure 6. Tracing back the mass build-up of the dark matter haloes as a function of expansion factor and redshift for both the X-ray fossils and the control groups 1 and 2. (a) For all haloes. (b) High mass haloes ($m_{\rm halo} \gtrsim 3.34 \times 10^{13}\, h^{-1}$ M$_\odot$). Both plots indicate the earlier formation of X-ray fossil groups in comparison to control groups. (c) Low mass haloes ($m_{\rm halo} \lesssim 3.34 \times 10^{13}\, h^{-1}$ M$_\odot$). Here the difference in evolution between the X-ray fossil and control groups is not as pronounced as in those seen in high mass X-ray fossils. All the masses are normalised to the mass at z=0.

exercise that is not directly possible to perform with observational surveys. In Fig. 6 we trace the mass evolution of present-day X-ray fossil systems backwards from $z = 0$, to $z = 0.82$ when the scale factor, a, of the Universe was 0.55 times its current size.

At any given redshift in Fig. 6 the average ratio of the mass of a halo to its final mass (at $z = 0$) is calculated for all eligible haloes. The error is represented by the standard error on the mean, i.e. $\sigma/\sqrt{N}$, where σ is the standard deviation of the original distribution and N is the sample size. The same was done for both sets of control groups. The original sample of fossils was divided into two subsamples, of low mass and high mass groups (see Fig. 6b and Fig. 6c), such that both subsamples have equal numbers of groups. The boundary between the two subsamples corresponds to the median present-day mass $\sim 3.34 \times 10^{13}\, h^{-1}$ M$_\odot$.

Fig. 6a shows that at a scale factor of 0.8 ($z \sim 0.24$), the fossil groups have already attained ~90% of their final mass while, at the same redshift, the fraction of assembled mass of the extreme non-fossil groups is about ~77% of their final mass. The intermediate control group gives intermediate values. The fossil groups have almost all their mass in place by a redshift of $z \sim 0.1$, and show no evidence of recent major mergers, while the non-fossils seem to be assembling mass even at the present day. These results suggest an early formation and consequent higher mass concentration in fossil groups, in comparison to normal groups, particularly for the more massive fossils.

As Figs. 6b and 6c show, the difference in mass assembly is larger in more massive haloes than haloes with lower mass. The decreased distinction in the assembly history for our lower mass fossil systems probably results from the fact there is a large fraction of "statistical fossils" in this category: groups which achieve $\Delta m_{12} \geqslant 2$ due to random chance, because of the small number of members. As can be seen in Fig. 3, ~50% of optical fossil groups with masses less than $\sim 3.3 \times 10^{13}\, h^{-1}$ M$_\odot$ are expected to fall into this "statistical fossil" category.

Various observational properties (Ponman et al. 1994; Jones et al. 2003; Khosroshahi, Jones & Ponman 2004; Ulmer et al. 2005; Khosroshahi et al. 2006; Khosroshahi, Ponman & Jones 2007) have suggested an early formation epoch for fossils. D'Onghia et al. (2005) and Sommer-Larsen (2006) used a set of twelve high-resolution numerical simulations in the ΛCDM cosmology to study the formation of fossil groups, and found a correlation for the magnitude gap between the brightest and second-brightest galaxies and the halo formation epoch, with fossils accreting half of their final dark matter mass at $z \geqslant 1$. Such an early assembly of fossil haloes leaves enough time for L_* galaxies to merge into the central one by dynamical friction, resulting in the observed magnitude gap at $z = 0$.

Fig. 7 shows the history of mass assembly of a typical example of a massive fossil group (right panel) and a control group (left panel) from the Millennium Gas Simulation from redshift $z = 1.0$ to $z = 0$. The dimension of each image is 10×10 Mpc, centred around the central halo. It can be seen that at $z = 0.3$, the X-ray fossil group has already largely been assembled, while the control group has considerable substructure even at a later epoch.

5 DISCUSSION

We studied the history of the mass assembly of fossil groups, selected using the usual observational criteria at $z = 0$, from a redshift $z = 0.8$ to the present day, within the Millennium simulation. A sample of X-ray fossil groups was defined from the Millennium simulations and associated gas and galaxy catalogues, according to the usual criteria: (a) the difference between the R-band magnitudes of the first and second ranked galaxies, within half the projected radius enclosing 200 times the mean density of material (R_{200}), is $\Delta m_{12} \geqslant 2$ magnitudes, and (b) The bolometric X-ray luminosity of the group is $L_{\mathrm{X,bol}} \geqslant 0.25 \times 10^{42} h^{-2}$erg s^{-1}. While optical fossil groups fulfill just the first condition, X-ray fossils satisfy both criteria. Our main results are as follows:

- The space density of X-ray fossil groups is in close agreement with the observed space density of fossils with $L_X > 2.5 \times 10^{42}$ h^{-2}erg s^{-1}. Although for low luminosity fossils we find roughly 1/3 of the observed fossil space density, there are several potential factors that could lead to this difference. As well as significant uncertainties in the observational studies, the X-ray properties of haloes in the real Universe show far greater scatter than those seen in the preheating simulation used here (Hartley et al. 2007). Given the X-ray luminosity threshold in the definition of an X-ray fossil, scatter in L_X will alter the X-ray fossil number density, since the number density of haloes is a steep function of mass.
- By selecting optical fossils from groups randomly generated from a Schechter luminosity function, we demonstrate that for small numbers of galaxies per group, a significant fraction of optical fossil groups are expected to be purely statistical, requiring no special physical mechanism to generate the 2 magnitude luminosity gap. For groups with more than 40 members, this effect largely disappears, with very few fossil groups expected at random.
- The probability of finding optical fossils with mass M, i.e, $P_f(M;\text{optical})$ is a decreasing function of: (a) group dark matter halo mass and, (b) the fraction of the virial radius within which the first and second brightest galaxies are being found. Conversely, as dark matter halo mass become small, the probability $P_f(M;\text{X-ray})$ for X-ray fossils decreases.
- Both high-mass and low-mass X-ray fossil groups are found to have assembled $\sim 90\%$ of their final masses by a redshift of $z = 0.24$. The corresponding mass fraction is about $\approx 70 - 80\%$ for two different sets of high-mass control samples, and $\approx 85\%$ for low-mass control samples, where groups fulfill the same X-ray luminosity criterion ($\gtrsim 3.34 \times 10^{14}\,h^{-1}\mathrm{M}_{\odot}$) but have the optical luminosity gaps corresponding $0.1 \leqslant \Delta m_{12} \leqslant 0.3$ and $0.8 \leqslant \Delta m_{12} \leqslant 1.0$ magnitudes.

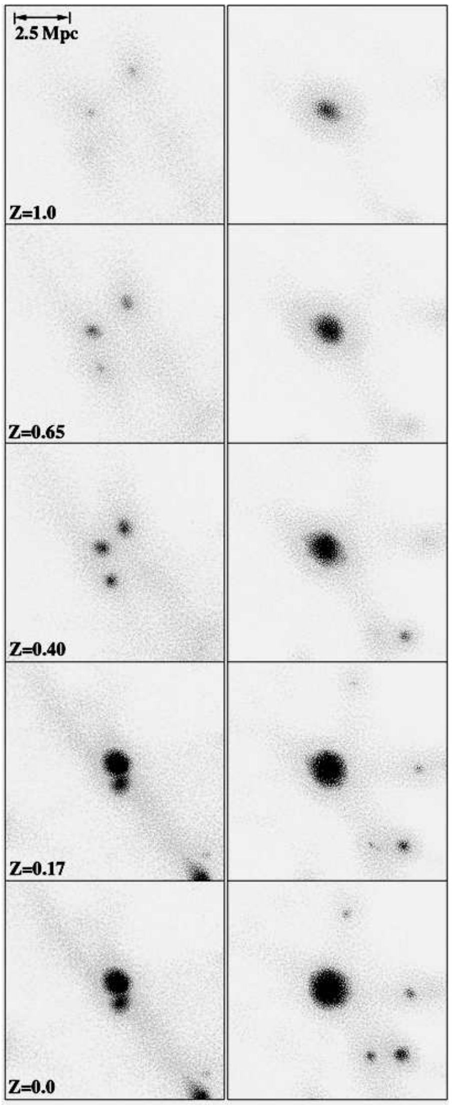

Figure 7. Evolution of a typical of massive X-ray fossil group (*right*) in comparison to a typical massive normal group (*left*) from redshift z=1.0 to 0. The dimension of each panel is 10 × 10 Mpc. The points represent individual gas particles from the Millennium Gas simulation (Pearce et al. 2007).

This study shows that fossils indeed are formed early, with more than $\sim$80% of their mass accumulated as early as 4 Gyr ago. They are also relatively isolated compared to non-fossils. The strongest X-ray fossil candidates are those with the highest X-ray luminosity as these systems are not expected to have a large luminosity gap between their first and second ranked galaxies entirely by chance. As always, systems with more than a handful of galaxies are to be preferred.

In principle, comparison of the observed space density of fossils as a function of X-ray luminosity with that of fossils from simulations can provide valuable constraints on the treatment of physical processes included in the simulations. The tentative evidence

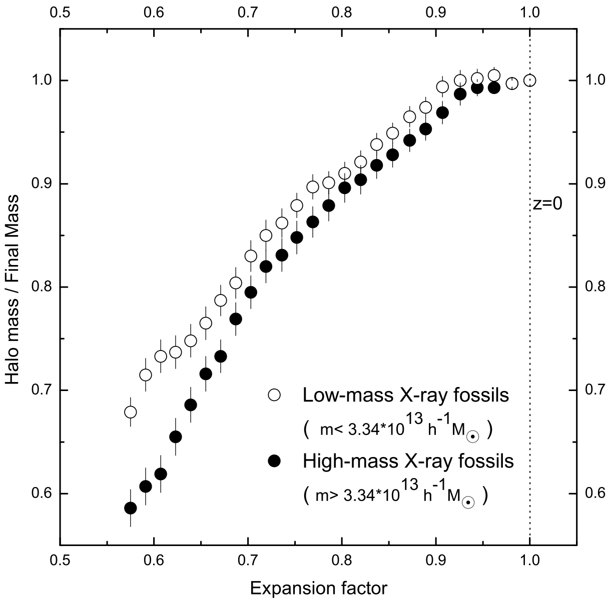

Figure 8. Comparison between the mass growth of high and low-mass X-ray fossils plotted in Figs. 6b and 6c.

for a discrepancy, whereby the observed space density of low X-ray luminosity fossil groups may exceed that predicted from the simulations, will be worth revisiting in the future, when better observational estimates are available.

It is interesting that while the amount of recent mass assembly in control groups increases with halo mass, as is expected in the hierarchical growth paradigm, there is almost no difference between the mass assembly of high-mass and low-mass X-ray fossils after redshift $z = 0.6$ (see Fig. 8). It seems that both low-mass and high-mass fossil systems are undisturbed at low redshift.

Since we expect faster orbital decay and more efficient galaxy merging in lower mass systems, due to the lower velocity dispersion of individual galaxies within the group, we would expect to find a higher incidence rate of fossils amongst poor groups. Fig.3 shows that this is indeed the case, but the effect is not very strong, once the influence of statistical fossils is removed, and in X-ray fossils any rising trend at low richness is overwhelmed by the fact that many of the optical fossils fail to exceed the X-ray luminosity threshold. A word of caution about the treatment of orbital decay is in order here. As discussed in Sec. 2.2, the orbital evolution of subhaloes in the Millennium simulation is well treated until these subhaloes are reduced by stripping to 20 dark matter particles, but thereafter is calculated semi-analytically, using an approximate formula. In practice, a significant fraction of the second ranked galaxies in the fossil systems we have extracted from the simulation have been stripped below this 20 particle limit. For example, in fossils with masses of only $10^{13}\,h^{-1}\,\mathrm{M}_\odot$, approximately 35% of second ranked galaxies have been stripped below the limit, though this fraction drops to ∼10% for systems with mass $>\ 10^{14}\,h^{-1}\,\mathrm{M}_\odot$. For such galaxies the timescale for their subsequent decay and merger with the central galaxy is not very reliable. However, this is not a major issue for massive haloes, and it is interesting and surprising that the incidence of fossils in rich systems is fairly flat at 3-4%. Observational studies should, in due course, show whether this is reflected in the real Universe. One example of a fairly rich fossil cluster has already been reported by Khosroshahi et al. (2006).

The magnitude gap distribution of haloes at different X-ray luminosities and the mass evolution of fossil groups discussed above both support the idea that X-ray fossil groups are not a distinct class of objects but rather that they are extreme examples of groups which collapse early and experience little recent growth, so that their galaxies have time to undergo orbital decay and merging. The X-ray and optical scaling properties of such extreme groups can be expected to differ from those of groups with more typical evolutionary histories, and such differences have already been observed (Khosroshahi, Ponman & Jones 2007). A comparison of such observed differences with the properties seen in the Millennium simulation groups is underway, and should provide a valuable check on the adequacy with which feedback processes and other baryon physics is handled in the simulations.

ACKNOWLEDGMENTS

The Millennium Simulation used in this paper was carried out by the Virgo Supercomputing Consortium at the Computing Centre of the Max-Planck Society in Garching. The semi-analytic galaxy catalogue is publicly available at http://www.mpa-garching.mpg.de/galform/agnpaper.

The Millennium Gas Simulations were carried out at the Nottingham HPC facility, as was much of the analysis required by this work. We would like to thank Arif Babul and Serena Bertone for the discussions on this topic.

REFERENCES

Allen, S.W., & Fabian, A.C., 1998 MNRAS, 297, L57
Arnaud, M,. & Evrard, A.E., 1999, MNRAS, 305, 631
Balogh, M.L., Babul, A, Voit, G.M., McCarthy, I.G., Jones, L.R., Lewis, G.F., & Ebeling, H., 2006, MNRAS, 366, 624
Barnes, J.E., 1989, Nature, 338, 123
Bond, J. R., Cole, S., Efstathiou, G. & Kaiser, N., 1991, ApJ, 379, 440
Borgani S., et al., 2006, MNRAS, 367, 1641
Colless, M. et al., 2001, MNRAS, 328 ,1039
Croton, D.J., Springel, V., White, S.D.M., De Lucia, G.; Frenk, C. S.; Gao, L.; Jenkins, A., Kauffmann, G., Navarro, J. F. & Yoshida, N., 2006, MNRAS, 365, 11
Cypriano, E.S., Mendes de Oliveira, C.L. & Sodré, L.Jr., 2006, AJ, 132, 514
D'Onghia, E., Sommer-Larsen, J., Romeo, A.D., Burkert, A., Pedersen, K., Portinari, L. & Rasmussen, J., 2005, ApJ, 630, L109
Dubinski, J., 1998, ApJ, 502, 141
Ebeling, H., Jones, L.R., Fairley, B.W., Perlman, E., Scharf, C., & Horner, D., 2001, ApJ, 548L, 23
Fellhauer, M., Kroupa, P., Baumgardt, H., Bien, R., Boily, C. M., Spurzem, R., & Wassmer, N., 2000, NewA, 5, 305
Hartley, W. et al., 2007, submitted MNRAS
Helsdon, S.F. & Ponman, T.J., 2000, MNRAS, 315, 356
Helsdon, S.F. & Ponman, T.J., 2003, MNRAS, 340, 485
Jeltema, T.E., Mulchaey, J.S., Lubin, L.M., Rosati, P., & Böhringer H., 2006, ApJ, 649, 649
Jones, L.R, Ponman, T.J., Horton, A., Babul, A., Ebeling, H. & Burke, D.J., & Forbes, D.A., 2003, MNRAS, 343, 627

Jones, L.R, Ponman, T.J. & Forbes, D.A., 2000, MNRAS, 312, 139

Khosroshahi, H.G., Jones, L.R. & Ponman, T.J., 2004, MNRAS,349, 1240

Khosroshahi, H.G., Maughan, B.J., Ponman, T.J. & Jones, L.R., 2006, MNRAS, 369, 1211

Khosroshahi, H.G., Ponman, T.J. & Jones, L.R., 2006, MNRAS, 372, L68

Khosroshahi, H.G., Ponman, T.J. & Jones, L.R., 2007, MNRAS, 377, 595

Kaiser, N., 1991, ApJ, 383, 104

Matsushita, K., 2001, ApJ, 547, 693

Mendes de Oliveira, C.L., Cypriano, E.S. & Sodré, L.Jr., 2006, AJ, 131, 158

Miles, T.A., Raychaudhury, S., Forbes, D.A., Goudfrooij, P., Ponman, T.J. & Kozhurina-Platais, V., 2004, MNRAS, 355, 785

Miller, C.J. et al., 2005, AJ, 130, 968

Milosavljević, M., Miller, C.J., Furlanetto, S.R. & Cooray, A., 2006, ApJ, 637, L9

Mulchaey, J.S. & Zabludoff, A.I., 1999, ApJ, 514, 133

Mulchaey, J.S. & Zabludoff, A.I., 1998, ApJ, 496, 73

Navarro, J.F., Frenk, C.S., & White, S.D.M., 1996, ApJ, 462, 563

Pearce, F. et al., 2007, submitted MNRAS

Ponman, T.J., Allan, D.J., Jones, L.R., Merrifield, M. & MacHardy, I.M., 1994 Nature, 369, 462

Ponman, T.J. & Bertram, D., 1993, Nature, 365, 51

Ponman, T.J., Bourner, P.D.J., Ebeling, H., & Bohringer, H., 1996, MNRAS, 283, 690

Romer A.K. et al., 2000, ApJS, 126, 209

Sales, et al., 2007, astro-ph:0706.2009v3

Schechter, P.L., 1976, ApJ, 203, 297

Spergel, D. N. et al., 2003, ApJS, 148, 175

Sommer-Larsen, J., 2006, MNRAS, 369, 958

Springel, V., White, S.D.M., Tormen, G. & Kauffmann, G., 2001, MNRAS, 328, 726

Springel, V. et al., 2005, Natur, 435, 629

Steinmetz, M., & White, S.D.M., 1997, MNRAS, 288, 545

Sun, M., Forman, W., Vikhlinin, A., Hornstrup, A., Jones, C. & Murray, S.S., 2004, ApJ, 612, 805

Tittley, E.R., Pearce, F.R., & Couchman, H.M.P., 2001, ApJ, 561, 69

Ulmer, M.P. et al., 2005, ApJ, 624, 124

Vikhlinin, A., McNamara, B.R., Hornstrup, A., Quintana, H., Forman, W., Jones, C. & Way, M., 1999, ApJ, 520L

White, D.A., Jones, C., & Forman, W., 1997, MNRAS, 292, 419

Xu, G., 1995, ApJS, 98, 355

Xue, H., Jim, G., & Wu, X.P, 2001, ApJ, 553, 78

Xue, Y.J, & Wu, X.P, 2000, ApJ, 538, 65

Yamagata T. & Maehara H., 1986, PASJ, 38, 661

Yoshioka, T., Furuzawa, A., Takahashi, S., Tawara, Y., Sato, S., Yamashita, K. & Kumai, Y., 2004, AdSpR, 34, 2525

van den Bosch, F.C., Yang, X., Mo, H.J., et al., 2007, MNRAS, tmp..139V

Vel*á*zquez, H., & White, S.D.M., 1999, MNRAS, 304, 254

Zabludoff, A.I. & Mulchaey, J.S., 1998, ApJ, 496, 39